Nanotechnology 15 (2004) S504–S511 PII: S0957-4484(04)77586-8

Dimensional metrology for nanometre-scale science and engineering: towards sub-nanometre accurate encoders

Ralf K Heilmann[1], **Carl G Chen, Paul T Konkola and Mark L Schattenburg**

Space Nanotechnology Laboratory, Center for Space Research, Massachusetts Institute of Technology, Cambridge, MA 02139, USA

E-mail: ralf@space.mit.edu

Received 8 March 2004
Published 23 July 2004
Online at stacks.iop.org/Nano/15/S504
doi:10.1088/0957-4484/15/10/002

Abstract

Metrology is the science and engineering of measurement. It has played a crucial role in the industrial revolution at the milli-inch length scale and in the semiconductor revolution at the micrometre length scale. It is often proclaimed that we are standing at the threshold of another industrial revolution, brought by the advent and maturing of nanotechnology. We argue that for nanotechnology to have a similarly revolutionary effect a metrology infrastructure at and below the nanometre scale is instrumental and has yet to be developed. This paper focuses on dimensional metrology, which concerns itself with the measurement of lengths and its applications such as pattern placement and feature size control. We describe our efforts to develop grating- and grid-based scales with sub-nanometre accuracy over 300 mm dimensions using the nanoruler—a scanning-beam interference lithography tool.

(Some figures in this article are in colour only in the electronic version)

1. Introduction

In today's world many engineers, scientists, and even consumers take the existence of, and adherence to, precise industrial standards as a given. These standards form the basis for the interchangeability and compatibility of mechanical and electrical components. However, at the beginning of the first industrial revolution in the middle of the 18th century the concept of interchangeable parts was practically unknown. Parts had to be laboriously ground to fit into an assembly. Only about a century later did this concept turn into reality. Interchangeability, in turn, was enabled by the existence and widespread dissemination of improved metrology artefacts and comparators such as standardized rules and affordable pocket vernier calipers, accurate at the milli-inch scale and below. Still several decades passed before pioneers such as Henry Ford and Thomas Alva Edison introduced the developed world to low-cost, industrial mass production for the final phase of the second industrial revolution at the beginning of the 20th century.

The invention of the integrated circuit (IC) by Kilby and Noyce in 1958 is often named as the beginning of the information age and the semiconductor revolution. Initially, the mechanical metrology infrastructure with its micrometre precision and accuracy was sufficient to support IC line widths which started at 200 μm. At about the same time the laser was invented, but it took another decade before Hewlett-Packard produced a commercial heterodyne laser interferometer, the first practical tool to control stage motion with interferometry and nanometre resolution. Since then the wavelength of visible laser light has become the *de facto* length standard at the core of the metrology infrastructure of the semiconductor industry. This allowed line widths to continue to shrink down to below 100 nm today. The interferometer also is instrumental in numerous other applications where sub-micron positional accuracy is required, such as coordinate measuring machines (CMMs) and diamond turning machines.

[1] Author to whom any correspondence should be addressed.

© 2004 IOP Publishing Ltd Printed in the UK

As these examples of previous industrial revolutions show, a mature and economic metrology infrastructure needs to be in place well before the confluence of new scientific discoveries, new technologies developed in laboratories, visionary ideas, and appropriate support from government can lead to comparable revolutionary industrial developments of global scale. It has been argued before that the metrology infrastructure required for a nanotechnology-based industrial revolution is yet to be established [1]. This is in accordance with the goals of the National Nanotechnology Initiative (NNI) which has identified 'Nanoscale Instrumentation and Metrology' as one of several Grand Challenge Areas that have 'the potential to realize significant economic, governmental, and societal impact' [2].

There is a multitude of parameters and properties (electrical, magnetic, optical, chemical, mechanical, biological, etc) that need to be characterized at nanometre spatial dimensions and below, such as composition, structure, conductivity, coercivity, and physical dimensions, just as there is a wealth of approaches on how to measure them. In this paper we concentrate on dimensional metrology. In the following we briefly describe shortcomings of current dimensional metrology and areas where these limitations already slow technological progress or will do so in the near future. To help solve this metrology problem we propose the fabrication of large-area gratings and grids with sub-nanometre phase accuracy. Below we discuss their usefulness as encoder scales with the potential to replace interferometer-based metrology frames, or as large-scale, sub-nanometre accuracy pitch standards. We have constructed a prototype grating fabrication tool based on the idea of scanning-beam interference lithography (SBIL), called the nanoruler. It is currently capable of patterning 300 mm diameter substrates with ~1 nm pattern placement repeatability. We describe its design and capabilities in section 4 before summarizing in section 5.

2. Limitations of dimensional metrology and affected applications

2.1. Limitations of the displacement measuring interferometer

Most modern high-precision tools that require ultimate accuracy over distances larger than a fraction of a millimetre, such as chip lithography and metrology equipment, coordinate measuring machines, diamond turning machines and the like, depend on the displacement measuring interferometer (DMI) for measuring the displacement of the stage that supports the sample or work piece.

Commercial DMIs typically have sub-nanometre resolution [3], but the practical precision and accuracy that can be achieved are usually far worse. DMIs are able to perform dimensional metrology to a precision approaching 200 nm (0.2 μm) in an ordinary laboratory or factory environment, ~10 nm in a well-controlled environment, and ~2 nm in a vacuum chamber. While this level is sufficient for patterning 100 nm features, it is insufficient for the measurement and control of features under 10 nm. The primary errors plaguing interferometers include environmental disturbances such as temperature, pressure and humidity fluctuations, atmospheric turbulence, position-dependent geometric errors and several optical and electronic non-linearities [4, 5]—errors that are difficult to eliminate due to the nature of interferometers.

Interferometers often utilize folded and time-varying beam paths which compromise accuracy, and result in large, bulky and expensive systems, especially when multiple degrees of freedom need to be measured (six or more is not uncommon). In addition, large and heavy reference mirrors must be affixed to the stage, increasing its size and mass, lowering its resonance frequency and thus increasing vibration, and requiring larger motors, which in turn increases heat loads. The increased vibration and heat compromise accuracy and lower throughput. We believe that DMIs are near their practical accuracy limit and that new approaches need to be considered for nanoscale manufacturing, whether in the semiconductor industry or elsewhere.

2.2. Pattern placement

The ability to place patterns with nanometre-scale features with ~1 nm accuracy or better, often over areas tens or hundreds of millimetres in size, is of increasing importance in a number of high-technology applications. Similarly, the National Science and Technology Council states that 'instrumentation for precise nanometre-position control across samples of centimetre dimensions will be required to realize commercial nanoscale device fabrication' [2]. In the following we describe some examples of applications that critically depend on nanometre or sub-nanometre level metrology precision or accuracy.

2.2.1. Integrated circuit fabrication. The semiconductor industry is determined to utilize its vast expertise and infrastructure in lithographic patterning to fabricate integrated circuits with ever smaller minimum feature sizes for years to come. These ICs are built up sequentially from many layers. The lithographically transferred patterns for each layer must be overlayed precisely for proper functioning of the final chip, which requires careful alignment of wafer and mask stages. The current International Technology Roadmap for Semiconductors [6] anticipates today's wafer overlay tolerance of 35 nm to shrink to 7.2 nm for 450 mm diameter wafer production within 15 years. Since the required wafer overlay metrology precision should be no worse than 10% of the tolerance, sub-nanometre metrology precision is required. It is interesting to note that when patterning takes place during scanning, as is the case with most current lithography step-and-scan systems, such high precision even requires the inclusion of relativistic corrections in order to interpret interferometer data correctly [7].

2.2.2. Microscopes and maskless pattern generators. Many types of dimensional metrology tools with sub-micron and in some cases sub-nanometre resolution are available today. Examples are optical and electron microscopes, and proximity probes such as scanning tunneling microscopes and atomic force microscopes. Similarly useful in nanoscale science and engineering are related maskless patterning tools such as electron and laser beam writers. However, in many of these tools the stage that holds the sample being measured

or patterned has an accuracy at least an order of magnitude worse than the probe resolution. And since the area accessible to the probe—often called the field—is typically only a few to a few hundred microns in size, larger areas are imaged or patterned by stitching together different fields obtained by moving the sample stage. Therefore stage inaccuracies lead to stitching errors at the field boundaries and make it difficult to locate features or characterize processing-induced changes. Probe deflection non-linearities within a field cause intra-field distortions and also contribute to stitching errors. A metrology frame with sub-nanometre accuracy over macroscopic length scales could reduce stage-limited inter-field errors and serve as a pitch standard to calibrate and subtract intra-field distortions. The feasibility of this idea has been demonstrated for electron beam writing in the form of spatial-phase-locked electron-beam lithography (SPLEBL), with resulting field-stitching errors and global placement accuracy relative to a fiducial grid of below 1.3 nm (1σ) [8].

2.2.3. Nanomagnetic media. Pattern placement metrology will also be crucial for the development of patterned magnetic recording media. Traditional continuous thin film magnetic recording media are required to support higher and higher bit densities, rapidly approaching the superparamagnetic limit where individual grains are so small that thermal energy alone allows them to reverse magnetization spontaneously, rendering them useless for long-time data storage. A much explored alternative to achieve higher bit densities is the use of media consisting of pre-patterned arrays of single-domain magnetic particles [9]. Thermally stable particles of less than 10 nm diameter are conceivable. However, in the case of spinning-disc systems synchronization between the read-and-write process and the position of individual magnetic particles with a pitch of 25 nm (160 Gbits cm^{-2}) already is predicted to require pattern edge jaggedness of $\sim$1 nm or less [10]. Certainly pattern placement metrology accuracy at the sub-nanometre level is desired.

2.2.4. Optoelectronic devices. Grating-based opto-electronic devices, such as Bragg grating channel add-drop filters, can serve as high-bandwidth optical switches [11]. Surface relief gratings on waveguides may be many millimetres long, but at the same time they require the grating lines to be placed accurately within 5 nm or better over the whole length for optimum performance. This exceeds the capabilities of the best commercial electron beam writers. And again, the underlying dimensional metrology needs to be accurate at the 1 nm level.

2.2.5. Templates for self-assembly. The ability of molecules to self-assemble into large and complex structures is one of nature's great lessons that researchers are only beginning to utilize. Self-assembly has been employed to create many systems with sub-micron scale features, such as self-assembled monolayers on solid (SAMs) and liquid (Langmuir monolayers) substrates. However, most of these systems are quasi-two-dimensional in nature, and therefore do not possess sufficient long-range order, but instead display ordered domains of limited size, separated by domain boundaries. A possible approach to macroscopically ordered self-assembly might involve the use of patterned templates as substrates [12, 13]. For example, surface relief gratings with a coarse period comparable to the diameter of ordered self-assembled domains could force molecules to assemble with long-range order due to the additional, substrate-imposed constraints. For optimum control of defects it is desirable to place the template pattern with an accuracy of a fraction of the nearest-neighbor distance of the assembling molecules. This can easily result in a 1 nm template accuracy requirement.

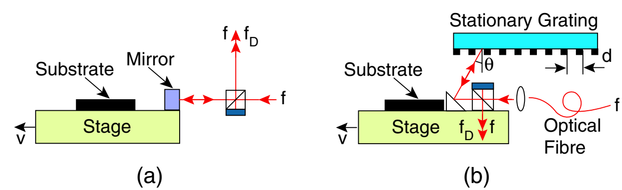

Figure 1. Schematic comparison between (a) displacement measuring interferometry and (b) optical encoder. A laser beam of frequency f is split in two by a beam splitter. In case (a) one beam traverses a variable distance to the stage, which moves with velocity v, and is reflected back with a Doppler-shifted frequency $f_D = f(1 - vn/c)$ before being superimposed with the stationary arm of frequency f. The index of refraction is n, and c is the velocity of light in vacuum. In case (b) the beam splitter is mounted to the moving stage. It sends one beam to the stationary grating, where it is diffracted back and undergoes a frequency shift $\Delta f = f - f_D = -f(vn/c)\sin\theta$. It is then superimposed with the other arm of frequency f. The geometrical path lengths between splitting and recombining the laser beam remain constant and independent of stage translation. The distance travelled through air can be made as short as a few hundred microns or less.

2.3. Coordinate measuring machines

Coordinate measuring machines play a crucial role in almost any kind of modern precision engineering on the macroscopic scale. The number of applications where large scale tools and parts need to be shaped, assembled, aligned and characterized with sub-micron precision and accuracy is steadily increasing. Some examples are the manufacture of large precision optical surfaces in general, or the diamond turning of assembly tooling for x-ray optics in astronomy in particular [14], where sub-micron accuracy is required over volumes of the order of 1 m^3. Even more demanding are the requirements for extreme ultraviolet (EUV) optics that offer an avenue to take semiconductor device fabrication to the 30 nm feature size level. Assembly tolerances are in the nanometre range, and the optic figure of the order of 0.1 nm [15]. Precision CMMs mostly rely on metrology frames based on laser interferometers and are therefore subject to the shortcomings discussed above (see section 2.1).

3. Optical encoders

Optical encoders have been used for decades as displacement measuring devices. In simple terms, an encoder consists of a scale and a scanning device that reads off the scale. Optical encoder scales are rigidly attached to a metrology frame and consist of grating or grid plates, and the read head—typically mounted to a moving stage—senses displacement relative to the grating scale (see figure 1). Highest resolution (a small

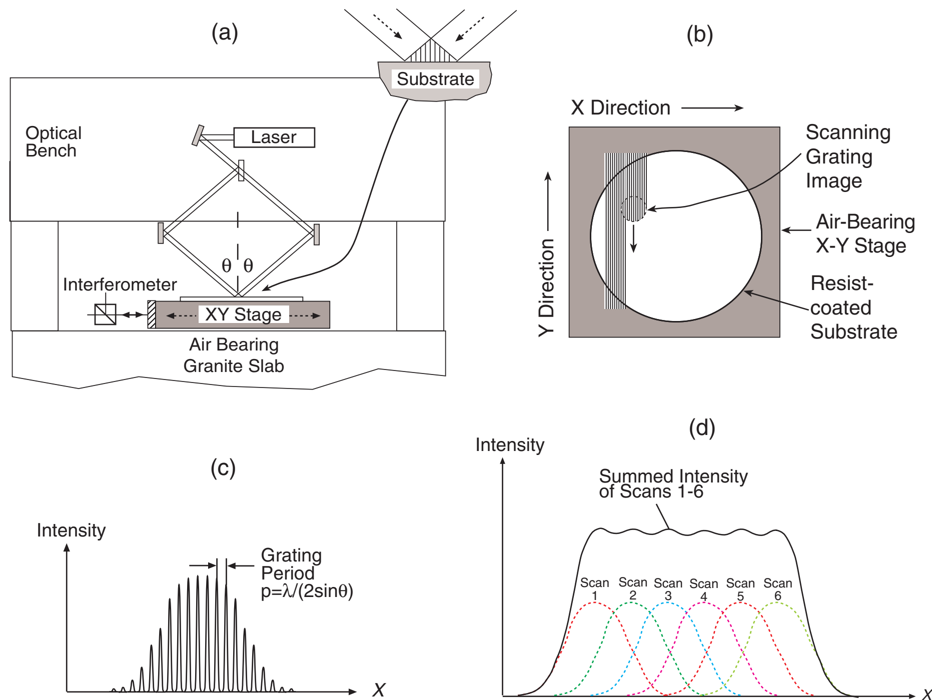

Figure 2. Schematic description of scanning-beam interference lithography. (a) Two Gaussian beams from a laser interfere at half-angle θ on the surface of a stage mounted substrate. The blow-up shows the standing wave interference pattern or interference fringes. (b) The whole resist-coated substrate is exposed by scanning the stage under the grating image. (c) Schematic intensity distribution within the interference region. (d) Desired dose uniformity in the resist is achieved through appropriate overlapping of subsequent scans.

fraction of the grating period) is achieved with a variety of diffraction-based schemes [16, 17]. The main advantages of optical encoders are the short and constant beam path lengths between gratings and sensors, reducing the effects of the atmosphere by orders of magnitude compared to laser interferometers. The use of optical encoders also allows one to replace the heavy interferometer stage mirrors required for DMIs with miniaturized encoder sensors, thereby increasing stage resonance frequency and reducing stage weight. The main problem with encoders today is that commercially available encoder plates have accuracies worse than ~100 nm over centimetre length scales. Even the best custom made scales are only accurate at the 100 nm level [18]. Since the encoder can only be as accurate as the grating scale, advance in this area crucially depends on the availability of encoder plates with sub-nanometre accuracy over macroscopic distances [19].

4. Towards nanometre-accurate grating fabrication with the nanoruler

Diffraction gratings are typically manufactured in one of two ways [20]. They are either mechanically ruled with a diamond tip, which is a very slow, expensive, and difficult to control process, especially for large gratings with fine periods, or the grating pattern is defined lithographically—typically by interference lithography (IL) or electron beam lithography (EBL)—in a resist layer and then chemically transferred into a substrate. IL is fast, but prone to hyperbolic distortions [21], while EBL patterns suffer from high frequency jitter and stitching errors and still take considerable time to write. Today neither one of these techniques is capable of producing linear gratings of many centimetres in size with sub-nanometre accuracy [19].

4.1. Scanning-beam interference lithography

Over the last several years our laboratory has developed a patterning tool with the above demands in mind. It is based on the technique of scanning-beam interference lithography (SBIL), which can be described as a hybrid between IL and mechanical ruling (see figure 2). Similar to IL, it uses the grating-like interference pattern ('image grating') generated at the intersection of two coherent laser beams to expose a resist-covered substrate. In contrast with IL, which often uses expanded spherical beams resulting in hyperbolic interference patterns, SBIL employs narrow, collimated beams of only ~1–2 mm diameter, resulting in an ultra-low-distortion image grating. Similar to mechanical ruling, the substrate is now scanned back and forth in serpentine fashion, with the interfering laser beams effectively acting as a scribe with thousands of 'tips' that rules thousands of lines in parallel. Due to the Gaussian nature of the laser beams it is necessary to overlap neighboring passes ('scans') sufficiently to achieve a uniform exposure dose on the substrate. The challenge for SBIL is to step over exactly by an integer multiple of the image grating period between scans, and to lock the image grating phase to the substrate reference frame during scanning in order to achieve straight grating lines in the resist with nanometre spatial phase coherence across the whole substrate.

4.2. The nanoruler

The nanoruler is an SBIL tool for the patterning and metrology of gratings in excess of 300 mm × 300 mm in size. The

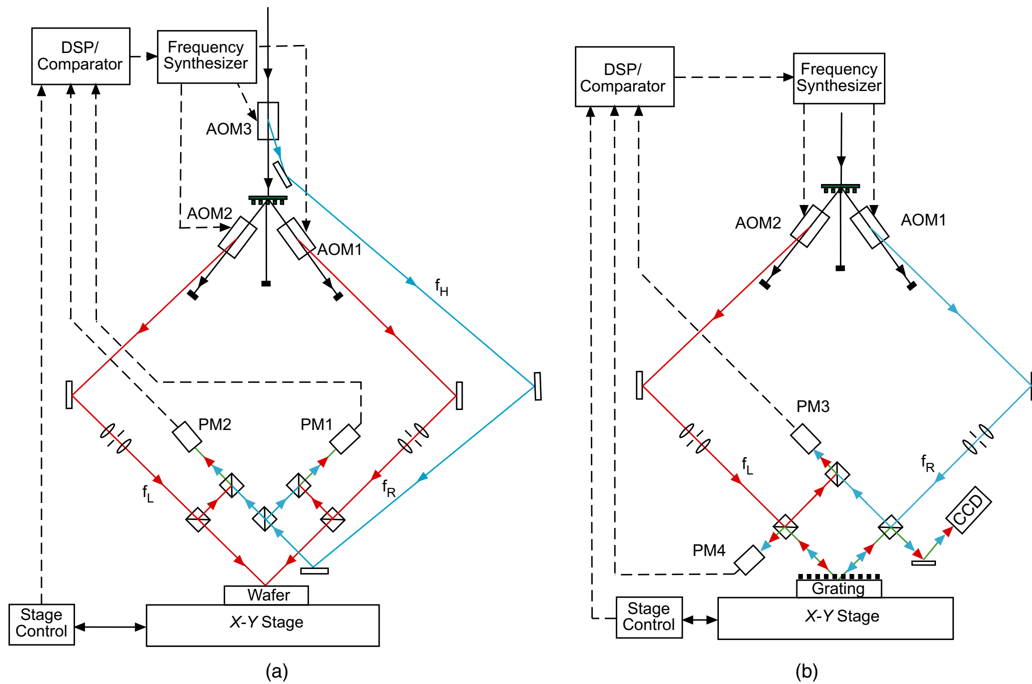

Figure 3. Schematics of nanoruler operational modes. (a) Writing or patterning mode: left arm (frequency f_L) and right arm (frequency f_R), which are both frequency shifted by 100 MHz via acousto-optic modulators AOM1 and AOM2, are partially picked off just before they interfere and combined with the diffracted output beam from AOM3, which operates at 120 MHz for heterodyning with a 20 MHz carrier frequency. The phase difference between phase meters PM1 and PM2 and the stage interferometer data are fed back into a digital comparator. The frequency synthesizer then adjusts the drive frequency for AOM1 to lock the phase of the image grating to the stage frame of reference. (b) Reading or metrology mode: a diffraction grating is taking the place of the substrate on the stage. AOM1 operates at a drive frequency of 90 MHz and AOM2 at 110 MHz. The feedback signal from phase meter PM3 and the stage interferometer are used to adjust the AOM1 frequency to generate a 20 MHz heterodyne signal at phase meter PM4, which measures the phase of the superposition of the reflected right arm and the -1 order of the left arm back-diffracted from the grating. Any deviation from the 20 MHz heterodyne frequency at PM4 is equivalent to a fringe-to-substrate motion in writing mode.

'metrology mode' allows the mapping or 'reading' of the spatial phase of existing gratings with the same accuracy as the gratings patterned in the 'writing mode' (see figure 3). The nanoruler sits on top of a massive granite block, which in turn is supported by an active vibration isolation system with added feed forward control to compensate for stage motion. On top of the granite block glides a motorized x–y air bearing stage with Zerodur mirrors and a Super Invar vacuum chuck. Stage position feedback is provided through a commercial heterodyne DMI system operating at a wavelength of $\lambda = 633$ nm.

Attached to the granite block is a vertical optical bench that holds numerous optics for interference lithography and metrology. The reading and writing interferometry employs a remotely operated Ar-ion laser with $\lambda = 351.1$ nm. The period p of the image grating is given by

$$p = \frac{\lambda}{2\sin(\theta)}, \qquad (1)$$

where θ is the half angle between the two interfering arms. The laser beam is locked to the frame of the optical bench through a beam steering system [22]. It is split into two arms with a grating beam splitter. The two arms are aligned with a computerized alignment system to interfere at the substrate at the desired angle [23]. The period of the image grating is verified interferometrically with a precision better than 3 ppm (3σ), or 1.1 pm for a period $p = 400$ nm [24, 25]. Distortions in the grating image are mapped through phase-shifting interferometry and can be minimized through the adjustment of spatial filter lenses in each arm [24, 25].

Just before the two beams interfere at the substrate a beam splitter picks off a fraction of the incident power in each arm. These beams, together with a frequency-shifted third arm for heterodyning, are guided through optical fibres to digital phase meters. The phase signals are used as feedback to lock out image fringe movement due to environmental disturbances. The fringe-locking optics are mounted on a single Zerodur metrology block, using a custom designed beam splitter and thermally balanced mounts to minimize phase differences between the image grating on the substrate and the phase measurement. The phase meter signal, together with stage DMI information, is fed back to a digital signal processor, which in turn instructs a custom digital frequency synthesizer that drives acousto-optic modulators in each lithography arm, thereby locking the image grating spatial phase to the moving substrate frame [26–28].

The fringe-to-substrate phase placement repeatability is the fundamental metric in the design of our current prototype [28]. Error sources that reduce repeatability can be grouped by subsystem (see table 1) or by their physical origin (see table 2). We distinguish between subsystems as follows. The stage DMI measures the displacement of the sample stage with respect to the column reference mirror, which is integrated into the metrology block. Repeatability

Table 1. Error budget summary by subsystems. The 'static' case refers to a thermally well equilibrated system with a short (<7 cm) interferometer dead path and no clamping distortions. The 'worst case' scenario applies to patterning a 300 mm substrate and includes additional thermal expansion errors from moving the stage through a thermal gradient, the longer dead path, and clamping distortions.

Error category	Error budget ('static') (±nm)	Error budget ('worst case') (±nm)
Displacement interferometer	1.66	4.88
Fringe locking interferometer	1.58	1.58
Metrology block frame	0.51	0.51
Substrate frame	0.40	2.83
Rigid body error motions	0.12	0.12
rss error	2.39	5.88

Table 2. Error budget summary grouped by physical origin for the 'worst case' scenario as described in table 1.

Error category	Error budget (±nm)
Thermal expansion	2.46
Air index variations	5.00
Periodic interferometer error	1.02
Electronic errors	0.22
Vibration	0.08
Substrate clamping distortion	1.41
Substrate thickness variation	0.50
Control loop	0.40
rss error	5.88

in this measurement is compromised by thermal expansion, air index variations, periodic interferometer errors, electronic errors, and inaccuracies in refractometer correction. Errors in the UV lithography interferometer are due to imperfections in the fringe-locking sensor signal and electronics, air index variations, periodic UV interferometer errors, and control loop performance. Metrology block errors describe thermal and vibration-induced motion of fringe-locking optics relative to the column reference mirror. Substrate frame errors consist of changes or imperfections in substrate location with respect to the stage mirror, which are due to vibrations, thermal effects, substrate clamping distortions, and substrate non-flatness. Rigid body error motions lead to errors due to relative motions between stage, metrology block, interferometer heads, and interferometer beams, and are dominated by Abbe errors.

The whole nanoruler is placed inside an environmental class 10 clean room enclosure that controls temperature fluctuations to within $\pm 0.005\,^{\circ}$C and humidity to within $\pm 1\%$. The enclosure, in turn, sits inside a larger temperature controlled class 100 clean room. In addition, slow, uniform variations in the index of refraction, such as those due to changes in pressure, humidity, and CO_2 levels, are corrected through the use of a refractometer close to the region of interference [27, 28].

Nevertheless, while writing we have no separate measure of inaccuracies in the stage DMI readings and small variations in the short optical paths between substrate and fringe-locking optics due to vibrations, distortions, and index variations. In reading mode, however, where the beam paths are practically identical to writing mode, we can also utilize our fringe-locking system and directly measure the remaining fringe-to-substrate displacement (see figure 3). This is achieved by heterodyne measurement of the phase in the superposition of the reflected (zero order) beam from one arm and the diffracted (minus first order) beam from the other arm. We can thus directly observe the fringe-to-substrate motion under conditions equivalent to writing mode. Typical fringe placement errors are on the order of 2.1 nm (3σ) [27, 28].

Probably the biggest advantage of the SBIL technique is the dose averaging that takes place in the resist due to scanning and overlapping exposures. This averaging greatly reduces the effect of any remaining image grating distortions, period measurement inaccuracies, and high-frequency fringe-to-substrate motion [24, 27, 28]. Experimentally we find grating mapping repeatability over a 100 mm diameter grating to be better than 3 nm (3σ) [27, 28]. Taking into account the attenuation of high frequency disturbances due to the dose averaging over 2 mm diameter beams during scanning at 100 mm s^{-1}, we expect dose placement stability of 2.1 nm (3σ). Furthermore, the effects of periodic DMI errors (observed to be of the order of 0.35 nm (1σ) in our system) could be averaged out to a large extent simply by scanning both stage axes in a manner that pushes these errors to high enough frequencies [28].

We have patterned 300 mm diameter substrates with a 400 nm period grating in about 20 min (see figure 4). Mechanically ruling the same grating would require a single diamond tip to travel more than 200 km, which would lead to excessive tip wear, and would take well over a month of continuous work under the best of circumstances.

So far our efforts have focused on achieving a high level of repeatability in the patterning of large-area gratings. We are currently investigating repeatable systematic errors, such as those due to stage mirror non-flatness or interferometer misalignment, to improve system accuracy. We believe that repeatability is primarily limited by remaining air index non-uniformity, thermal expansion effects, and periodic stage interferometer non-linearities (see also table 2). Detailed error analysis tells us that reduced temperature gradients, wider use of lower expansion materials such as Zerodur, possible vacuum enclosure of a stage interferometer arm, and scanning strategies that minimize periodic DMI errors will allow grating patterning and mapping repeatability well under 1 nm (3σ) [28].

5. Summary and outlook

As with past industrial revolutions, the nanotechnology revolution depends on the existence of a capable and economical metrology infrastructure before it can proceed swiftly. This infrastructure is currently not in place. In the area of macroscopic dimensional metrology the shortcomings of displacement measuring interferometry can be overcome through the employment of optical encoder schemes that utilize nanometre precise and accurate encoder plates. We have introduced scanning-beam interference lithography as a promising technique for the fabrication of such encoder plates. With the nanoruler, our prototype SBIL tool, we have so far demonstrated pattern placement control and mapping repeatability better than 3 nm (3σ) and expect further improvement. Ultimately, the DMI-based stage control itself

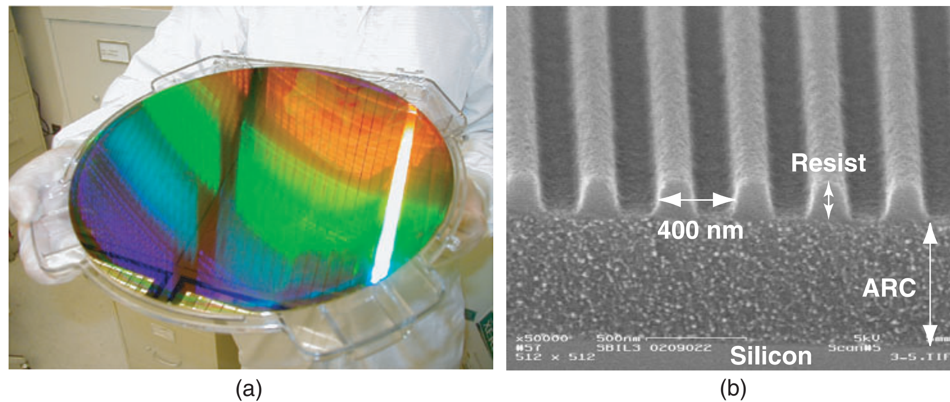

Figure 4. (a) A 300 cm diameter silicon wafer patterned in the nanoruler with a 400 nm period grating. Overhead fluorescent lighting and the camera flash diffract off the grating. (b) Scanning electron micrograph of a resist grating on an anti-reflection coated (ARC) silicon wafer after exposure in the nanoruler and development.

will be replaced by accurate, stable, calibrated encoders that allow traceability to length standards. In the future, encoder grids (i.e. two orthogonal gratings for metrology in two dimensions) can be patterned either through double exposure of a substrate with exact 90° substrate rotation between exposures, or through extension of the current system from two to four interfering beams. As we have demonstrated, large-area encoder plates can be patterned in less than an hour, which holds the promise of inexpensive high-volume production. In addition various methods of grating or grid replication could lower the price of such encoder plates even more, assuming the replication process can be controlled well enough to keep distortions at the sub-nanometre level over all relevant length scales. Furthermore we believe that it will be possible to add the ability to vary the period and orientation of the image grating during scanning [29] to generate accurately chirped or curved gratings for applications in spectroscopy and optoelectronic devices.

Acknowledgments

We are grateful for the outstanding technical and facility support from R C Fleming, the Space Nanotechnology Laboratory, and the Nanostructures Laboratory. The 300 mm diameter gratings were patterned by J C Montoya. RKH acknowledges helpful conversations with T W Zeiler. This work was supported through grants from NASA and DARPA.

References

[1] Schattenburg M L and Smith H I 2001 Nanostructure science, metrology, and technology *Proc. SPIE* **4608** 116

[2] National Nanotechnology Initiative 2004 Research and development supporting the next industrial revolution supplement to the President's FY budget, National Science and Technology Council http://www.ostp.gov/NTSC/html/NTSC_Home.html

[3] Demarest F C 1998 *Meas. Sci. Technol.* **9** 1024

[4] Bobroff N 1993 *Meas. Sci. Technol.* **4** 907

[5] Teague E C 1993 *SPIE Institutes for Advanced Optical Technologies Series IS-10* ed C Marrion (Bellingham, WA: SPIE Optical Engineering Press) p 322

[6] International Technology Roadmap for Semiconductors http://public.itrs.net/

[7] Heilmann R K, Konkola P T, Chen C G and Schattenburg M L 2000 *J. Vac. Sci. Technol.* B **18** 3277

[8] Smith H I, Hector S D, Schattenburg M L and Anderson E H 1991 *J. Vac. Sci. Technol.* B **9** 2992
Hastings J T, Zhang F and Smith H I 2003 *J. Vac. Sci. Technol.* B **21** 2650

[9] Ross C A 2001 *Annu. Rev. Mater. Res.* **31** 203

[10] Nair S K and New R M H 1998 *IEEE Trans. Magn.* **34** 1916

[11] Lim M H, Murphy T E, Ferrera J, Damask J N and Smith H I 1999 *J. Vac. Sci. Technol.* B **17** 3208

[12] Cheng J Y, Ross C A, Thomas E L, Smith H I and Vancso G J 2003 *Adv. Mater.* **15** 1599

[13] Segalman R A, Hexemer A and Kramer E J 2003 *Macromolecules* **36** 6831

[14] Podgorski W A *et al* 2004 Optics for EUV, x-ray, and gamma-ray astronomy *Proc. SPIE* **5168** 318
Owens S M, Hair J, Stewart J, Petre R, Zhang W, Podgorski W, Glenn P, Content D, Saha T and Nanan G 2004 *Proc. SPIE* **5168** 239

[15] Goldberg K A, Naulleau P, Batson P, Denham P, Anderson E H, Chapman H and Bokor J 2000 *J. Vac. Sci. Technol.* B **18** 2911

[16] Teimel A 1992 *Prec. Eng.* **14** 147

[17] Jourlin Y, Jay Y and Parriaux O 2002 *Prec. Eng.* **26** 1

[18] Bosse H, Hässler-Grohne W, Flügge J and Köning R 2003 Recent developments in traceable dimensional measurements II *Proc. SPIE* **5190** 122
Bosse H, Hässler-Grohne W, Flügge J and Köning R 2003 *Metrologia* **40** 04002 (Techn. Suppl.)

[19] Schattenburg M L, Chen C, Everett P N, Ferrera J, Konkola P and Smith H I 1999 *J. Vac. Sci. Technol.* B **17** 2692

[20] Loewen E G and Popov E 1997 *Diffraction Gratings and Applications* (New York: Dekker)

[21] Ferrera J, Schattenburg M L and Smith H I 1996 *J. Vac. Sci. Technol.* B **14** 4009

[22] Konkola P T, Chen C G, Heilmann R K and Schattenburg M L 2000 *J. Vac. Sci. Technol.* B **18** 3282

[23] Chen C G, Heilmann R K, Joo C, Konkola P T, Pati G S and Schattenburg M L 2002 *J. Vac. Sci. Technol.* B **20** 3071

[24] Chen C G 2003 Beam alignment and image metrology for scanning-beam interference lithography—fabricating gratings with nanometer phase accuracy *PhD Thesis* Department of Electrical Engineering and Computer Science, Massachusetts Institute of Technology, Cambridge, MA http://snl.mit.edu/papers/theses/2003/cgc_phd_thesis.pdf and http://theses.mit.edu/

[25] Chen C G, Konkola P T, Heilmann R K, Joo C and Schattenburg M L 2002 Nano- and microtechnology:

materials, processes, packaging, and systems *Proc. SPIE* **4936** 126

[26] Heilmann R K, Konkola P T, Chen C G, Pati G S and Schattenburg M L 2001 *J. Vac. Sci. Technol.* B **19** 2342

[27] Konkola P T, Chen C G, Heilmann R K, Joo C, Montoya J C, Chang C-H and Schattenburg M L 2003 *J. Vac. Sci. Technol.* B **21** 3097

[28] Konkola P T 2003 Design and analysis of a scanning-beam interference lithography system for patterning gratings with nanometer-level distortions *PhD Thesis* Department of Mechanical Engineering, Massachusetts Institute of Technology, Cambridge, MA http://snl.mit.edu/papers/theses/2003/ptk-phdthesis.pdf and http://theses.mit.edu/

[29] Schattenburg M L, Chen C G, Heilmann R K, Konkola P T and Pati G S 2002 Optical spectroscopic techniques and instrumentation for atmospheric and space research IV *Proc. SPIE* **4485** 378
Pati G S, Heilmann R K, Konkola P T, Joo C, Chen C G, Murphy E and Schattenburg M L 2002 *J. Vac. Sci. Technol.* B **20** 2617